MOLECULAR AND CELLULAR BIOLOGY, Oct. 2004, p. 8970–8980 Vol. 24, No. 20
0270-7306/04/$08.00+0 DOI: 10.1128/MCB.24.20.8970–8980.2004

Glycogen Synthase Kinase 3 Phosphorylates RBL2/p130 during Quiescence

Larisa Litovchick, Anton Chestukhin, and James A. DeCaprio*

Dana-Farber Cancer Institute, Boston, Massachusetts

Received 11 May 2004/Returned for modification 9 June 2004/Accepted 22 July 2004

Phosphorylation of the retinoblastoma-related or pocket proteins RB1/pRb, RBL1/p107, and RBL2/p130 regulates cell cycle progression and exit. While all pocket proteins are phosphorylated by cyclin-dependent kinases (CDKs) during the G_1/S-phase transition, p130 is also specifically phosphorylated in G_0-arrested cells. We have previously identified several phosphorylated residues that match the consensus site for glycogen synthase kinase 3 (GSK3) in the G_0 form of p130. Using small-molecule inhibitors of GSK3, site-specific mutants of p130, and phospho-specific antibodies, we demonstrate here that GSK3 phosphorylates p130 during G_0. Phosphorylation of p130 by GSK3 contributes to the stability of p130 but does not affect its ability to interact with E2F4 or cyclins. Regulation of p130 by GSK3 provides a novel link between growth factor signaling and regulation of the cell cycle progression and exit.

Control of the cell cycle relies on the precisely regulated expression of the genes required for the cell cycle progression. The pocket proteins, including RB1/pRb, RBL1/p107, and RBL2/pRb2/p130, play overlapping but distinct roles in the regulation of the cell cycle (6, 7, 36). pRb, p107, and p130 share significant homology with each other, especially in two domains (A and B; see Fig. 1A) that together form the pocket domain critical for interaction with E2F transcription factors and viral oncoproteins, including adenovirus E1A and simian virus 40 (SV40) large T antigen (14, 18, 35, 56). Pocket protein binding to E2F results in active repression of E2F-dependent genes that are required for DNA synthesis and cell cycle progression as well as differentiation and DNA damage checkpoints (3, 53). Overexpression of retinoblastoma family members leads to E2F repression and cell cycle arrest, while phosphorylation of pocket proteins by cyclin-dependent kinases (CDKs) during G_1 and S phases results in dissociation from E2Fs and activation of E2F-dependent gene transcription (22). Interaction of pocket proteins with viral oncoproteins also leads to a loss of E2F binding and repression, providing an important mechanism for virus-mediated transformation (23, 56, 59).

Unique functional roles for each pocket protein are suggested by differential expression during the cell cycle and preferential binding to specific E2Fs. For example, the p130 protein level is elevated in quiescent cells and decreased in proliferating cells, while p107 is absent in quiescent cells and elevated in growing cells (52). While pRb has the strongest affinity for E2F1, E2F2, and E2F3, p130 and p107 preferentially bind to E2F4 and E2F5 (17). Complexes containing p130 and E2F4 and E2F5 are the most abundant pocket protein-E2F complexes in quiescent cells, whereas p107 and E2F4 complexes are predominant in proliferating cells (51). While these observations implicate p130 in the induction or maintenance of the quiescent state in normal cells, the genetic inactivation of all three retinoblastoma family members is required for complete loss of G_1 checkpoint in mouse embryonic fibroblasts (MEFs) (11, 48). In contrast, MEFs prepared from mouse strains with single- or double-knockout members of the retinoblastoma family members were capable of exiting from the cell cycle upon serum deprivation and contact inhibition (8, 29). These results suggested that pocket proteins can substitute for each other in cell cycle control and E2F regulation.

This functional redundancy in cell cycle control does not extend to the developmental regulation by the retinoblastoma family. While the homozygous deletion of the *Rb1* gene results in the embryonic death at mid-gestation, deletion of either p107 or p130 alone does not affect the development and viability of mouse embryos (reviewed in reference 40). Homozygous deletion of both p107 and p130 allowed the full-term development of the embryo but induced abnormalities of the cartilage, bone, and skin, contributing to neonatal lethality (8, 34, 45, 46). This observation suggests that despite overlapping functions in the cell cycle regulation, pRb, p107, and p130 play unique roles in development. Interestingly, deletion of p130 gene in the BALB/c strain resulted in embryonic lethality at midgestation, and a deletion of the p107 gene in this genetic background also caused severe developmental abnormalities that were not observed in mixed-genetic-background mice (31, 32). These differences in the knockout mouse phenotype could be attributed to the reported inactivating allelic variations of CDKN2A, the p16 CDK inhibitor 2A gene, that are found in the BALB/c mouse strain (60, 61).

Unlike pRb and p107, p130 is specifically phosphorylated in growth-arrested and in terminally differentiated cells (4, 22, 38). Notably, the p130 G_0 kinase has not been identified (37). Mass spectroscopy analysis of p130 purified from serum-starved cells revealed a highly phosphorylated region within the B box of the pocket (Fig. 1A) (4, 26, 27). This region spans residues 935 and 1000 of human p130 and is referred to here as the Loop. The Loop region has no sequence homology with the corresponding fragments of p107 and pRb. Earlier reports demonstrate that the Loop region contains a functional nu-

* Corresponding author. Mailing address: Dana-Farber Cancer Institute, Mayer 457, 44 Binney St., Boston, MA 02115. Phone: (617) 632-3825. Fax: (617) 632-4760. E-mail: james_decaprio@dfci.harvard.edu.

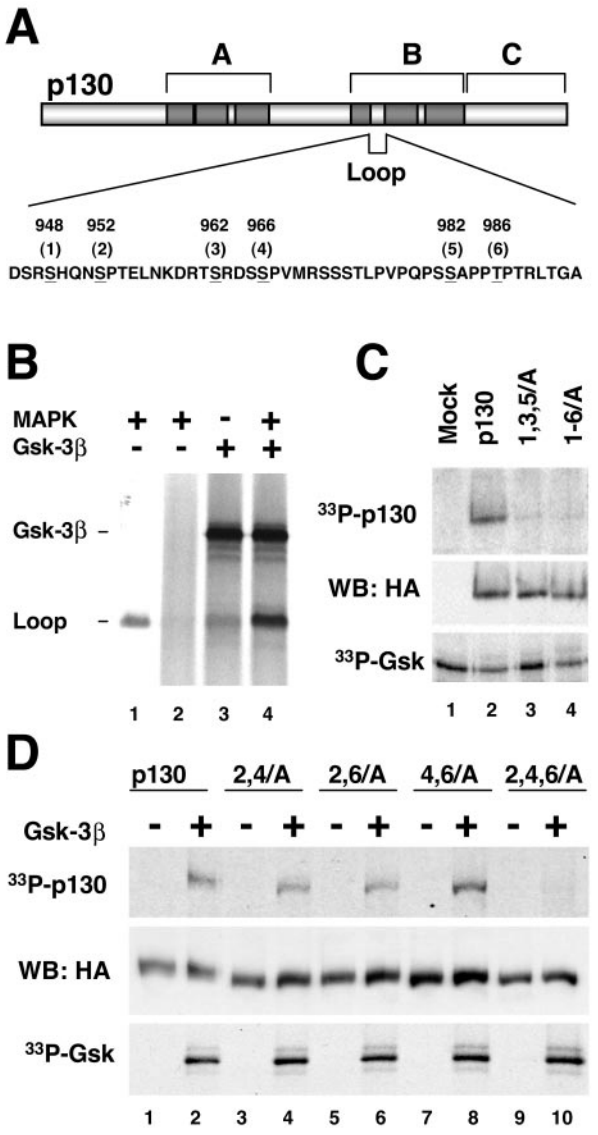

FIG. 1. Unique region of p130 contains three potential GSK3 phosphorylation sites. (A) Schematic structure of p130. The regions forming a pocket domain that is highly conserved among retinoblastoma family proteins are shown darkly shaded. The Loop region in the B-box of p130 is absent in pRb and has no homology with the corresponding region of p107. Residues matching the GSK3 phosphorylation consensus sequence are underlined. Positions of the sites (numbered from 1 to 6 for convenience) correspond to human p130. (B) GSK3 phosphorylates the Loop of p130 in vitro and requires priming phosphorylation. The GST-tagged S935-E1000 fragment (Loop) of p130 was absorbed on glutathione Sepharose beads and subjected to GSK3B (Gsk-3β) phosphorylation in the presence of [γ-^{33}P]ATP either directly (lane 3) or after priming phosphorylation with purified MAPK and nonradioactive ATP followed by extensive washing of the beads (lane 4). A control reaction with MAPK1-prephosphorylated GST-Loop but without GSK3B shows that phosphorylation is mediated by GSK3B and not by residual MAPK1 activity (lane 2). Lane 1 demonstrates phosphorylation of GST-Loop by MAPK1 in the presence of [γ-^{33}P]ATP. An autoradiogram shows phosphorylation of GST-Loop and autophosphorylation of GSK3B. (C) GSK3 phosphorylates p130 but not the 1,3,5/A or 1-6/A p130 mutants. HA-tagged p130 and the mutants were expressed in U-2 OS cells, immunoprecipitated, and incubated with purified GSK3B in the presence of [γ-^{33}P]ATP. An identically prepared sample from vector-transfected cells was used as a control (Mock, lane 1). Reaction products were resolved by SDS-PAGE (10% polyacrylamide gel), transferred to nitrocellulose, and subsequently analyzed by autoradiography and Western blot. The top and bottom panels show the autoradiograms of p130 phosphorylation and GSK3B autophosphorylation, respectively. The middle panel shows a Western blot with anti-HA antibody (WB: HA) confirming that comparable amounts of p130 and the mutants were present in each reaction. (D) GSK3 phosphorylates each of the three pairs of phosphorylation sites in the Loop region of p130. HA-tagged wild-type p130, 2,4/A, 2,6/A, and 4,6/A double mutants and the 2,4,6/A triple mutant were expressed and subjected to GSK3B phosphorylation as described for panel C. For each of the samples, a control reaction without GSK3B indicates that the phosphorylation is mediated by GSK3B and not by other p130-associated kinases (odd lanes). Reaction products were resolved by SDS-PAGE (10% polyacrylamide gel) and transferred to nitrocellulose. The top and bottom panels show the autoradiograms of p130 phosphorylation and GSK3B autophosphorylation, respectively. The middle panel shows a Western blot with anti-HA antibody confirming comparable amounts of p130 and the mutants were present in each reaction.

clear localization sequence and was not required for the growth suppression function of p130 (5, 26). Three pairs of phosphorylated residues in the loop (S948 and S952, S962 and S966, and S982 and T986 in human p130 sequence) matched the consensus pS-X-X-X-pS/pT-P, where X is any residue (Fig. 1A). Importantly, priming phosphorylation of the serine or threonine residue at the 0 position was required for phosphorylation of the corresponding serine residue at the −4 position (26). While the priming phosphorylation of S952 and T986 was most likely mediated by CDK2, phosphorylation of S948, S962, S966, and S982 was CDK independent (26).

Glycogen synthase kinase 3 (GSK3) is a ubiquitously expressed serine-threonine kinase implicated in diverse biological processes, including embryonic development, metabolism, specific gene transcription, and cytoskeleton function (reviewed in references 20, 43, and 57). Notably, GSK3 has been shown to phosphorylate serine or threonine residues at the −4 position after priming phosphorylation of S or T at the 0 position for several substrates in vivo (21, 44, 55). Mammalian GSK3 exists as two isoforms, GSK3A and GSK3B, that share 98% homology in their catalytic domain and have similar biochemical properties. Notably, GSK3 kinase activity is high in resting and nutrient-deprived cells and is negatively regulated upon activation of insulin receptor and Wnt signaling pathways (reviewed in reference 57). Deregulation of these pathways has been implicated in the pathogenesis of human diseases such as type II diabetes and cancer, making GSK3 an important target for biological and pharmacological studies. Here, GSK3 is shown to phosphorylate p130 at specific residues in the Loop region. Our results demonstrate that GSK3 phosphorylation of p130 could be an indication of a unique potentially important function of this retinoblastoma family member.

MATERIALS AND METHODS

Plasmids and recombinant retroviruses. Mutants of p130 were generated by two-step PCR with two overlapping mutagenesis primers (1) using *Pwo* DNA polymerase (Roche Biochemicals). The 5′- and 3′-flanking primers used for all constructs had the following sequences, respectively: F1, 5′CTTCGG GATCTCTGTGCC; and F2, 5′ATAGGGCCCTCTAGATGCATTAAA. Initially, a human p130 cDNA with a silent mutation disrupting an EcoRI site at position 2919 was generated by two-step PCR mutagenesis. This cDNA was then used as a template for PCR to generate p130 phosphorylation site mutants as follows. Fragments of 945 bp with the desired mutations were generated by PCR

with F1 and F2, digested with EcoRI, and inserted into the EcoRI-digested hemagglutinin (HA)-p130/pcDNA 3.1/Zeo expression vector (5). Orientation of inserts was determined by PCR, and mutations were verified by automated DNA sequencing.

To generate retroviral expression vectors, the verified p130/pcDNA3.1 constructs were digested with Bst1107 and ApaI and then inserted into appropriately digested HA-p130/pBabe-Puro vector (provided by H. Land). Recombinant ecotropic retroviruses were produced in Bosc 23 cells transfected with the corresponding pBabe-Puro plasmids (42), harboring p130 inserts as previously described (5, 39).

Cell lines and manipulations. U-2 OS, T98G, and NIH 3T3 cell lines were obtained from American Type Culture Collection and cultured in Dulbecco's modified Eagle's medium supplemented with 10% fetal bovine serum (FBS), 100-U/ml penicillin, and 100-μg/ml streptomycin (Invitrogen). BJ/hTert immortalized human fibroblasts were provided by W. Hahn. To generate U-2 OS-Eco and T98G-Eco cell lines stably expressing murine ecotropic receptor, U-2 OS and T98G cells were transfected with pEcoR/IRES-Neo plasmid (obtained from R. Scully) and selected in G418 (0.4 mg/ml; Gibco).

Cell lines expressing recombinant human p130 and mutants were created by infecting NIH 3T3, U-2 OS-Eco, or T98G-Eco cells with the corresponding recombinant retroviruses followed by antibiotic selection. For induction of G_0/G_1 growth arrest, cells were plated at 50% confluency and incubated in serum-free medium for 72 h. To stimulate entry into the cell cycle, fetal calf serum (20% final concentration) was added to the serum-starved cells. For in vivo inhibition of GSK3, the serum-starved cells were incubated with lithium acetate (47), GSK3 inhibitor II (Calbiochem), SB-216763, or SB-415286 (Biomol). Cell fractionation, flow cytometric analysis of the cell cycle profile, and immunofluorescent cell staining were performed as previously described (5).

Immunoprecipitations and Western blots. Cell extracts for immunoprecipitations and Western blots were prepared in EBC buffer (50 mM Tris-HCl [pH 8.0], 120 mM NaCl, 0.5% Nonidet P-40) supplemented with protease inhibitors (Set I; Calbiochem). The protein concentration of extracts was determined with the D_C protein assay (Bio-Rad). For in vitro phosphatase experiments, 100 μg of cell extract was incubated for 15 min at 30°C with 100 U of λ-phosphatase (NEB) in a buffer provided with the enzyme. For detection of proteins with phospho-specific antibodies and for the cycloheximide chase assay, cell extracts were prepared by lysis in sodium dodecyl sulfate-polyacrylamide gel electrophoresis (SDS-PAGE) loading buffer (60 mM Tris-HCl [pH 6.8], 2% SDS, 10% glycerol) and immediately boiled for 5 min. Typically, 30 μg of whole-cell extract was loaded in the gel for Western blot analysis and 1 mg of the extract was used for immunoprecipitation experiments.

Antibodies. The following antibodies were used for Western blot analysis: rabbit antibodies to p130 (C-20), E2F4 (C-108), p107 (C-18), and cyclin A (H-432) and mouse monoclonal antibody to cyclin E (HE12) (all from Santa Cruz); mouse monoclonal antibody to HA epitope (HA-11) (Covance); rabbit antibodies to phospho-S9-GSK3B (Cell Signaling Technology); and mouse monoclonal antibody to GSK3B (Upstate Biotechnology). Rabbit antibodies to HA epitope (Y-11) from Santa Cruz and mouse monoclonal antibodies to HA epitope (clone 12CA5) and SV40 large T antigen (clone PAb419) were used for immunoprecipitations. The ppRb2 rabbit polyclonal antibodies to diphosphorylated synthetic peptide NH_2-LPVPQPSpSAPPpTPTRLTGA, corresponding to residues 975 to 993 of human p130, were generated and affinity purified by Bethyl Laboratories, Inc.

In vitro phosphorylation assays. A glutathione *S*-transferase (GST)-tagged S935-E1000 fragment of p130 (GST-Loop) was expressed in *Escherichia coli* (DH5α), extracted with B-PER reagent (Pierce), and absorbed on glutathione-Sepharose beads. Washed beads were split into four aliquots and treated as follows. Two aliquots were incubated for 30 min at 30°C with 100 μM ATP, 20 U of p42 mitogen-activated protein kinase 1 (MAPK1; NEB), and 1× MAPK buffer (NEB), and one aliquot was incubated with an identical reaction mixture containing 10 μCi of [γ-^{33}P]ATP (NEN). Beads from two nonradioactive MAPK1 reaction mixtures were then washed three times with 50 mM Tris HCl buffer (pH 7.5) containing 150 mM NaCl and 10 mM EDTA and once with kinase buffer (20 mM Tris HCl buffer [pH 7.5], 10 mM $MgCl_2$, 5 mM dithiothreitol). The remaining aliquot of the beads and one of the nonradioactive MAPK1 reaction mixtures were then incubated for 30 min at 30°C with reaction mixture containing 100 μM ATP, 10 μCi of [γ-^{33}P]ATP, 25 U of GSK3B (NEB), and 1× GSK3 buffer (NEB). The second nonradioactive MAPK1 reaction mixture was incubated with an identical reaction mixture but without GSK3B to control for removal of MAPK1. Reactions were stopped by adding SDS-PAGE loading buffer and analyzed by SDS-PAGE and autoradiography.

For in vitro kinase assays with the full-length p130, cells were extracted with SDS-PAGE loading buffer to disrupt protein complexes and then diluted 10-fold with EBC buffer before immunoprecipitation of p130. Immunoprecipitates were washed three times with EBC and once with kinase buffer (20 mM Tris HCl buffer [pH 7.5], 10 mM $MgCl_2$, 5 mM dithiothreitol) and then incubated for 1 h at 30°C in a reaction mixture containing kinase buffer supplemented with 100 μM ATP and 2 μCi of [γ-^{33}P]ATP per ml in the presence or absence of 25 U of purified GSK3B (NEB).

Cycloheximide chase assay. Exponentially growing U-2 OS cells expressing HA epitope-tagged p130 or the indicated phosphorylation site mutants were plated onto six-well plates 24 h before the experiment. The cells were incubated with 30 μg of cycloheximide per ml and 25 μM MG132, as indicated in Fig. 5B. At indicated time points, the cells were rinsed with phosphate-buffered saline and extracted with SDS-PAGE loading buffer. An equal amount of protein extracts was loaded in the gel, and the expression of p130 and mutants was analyzed by SDS-PAGE followed by Western blot with anti-HA antibody. The intensity of the protein bands on the Western blot was quantified with Fluor-S MultiImager and Quantity One software (Bio-Rad). The same membranes were reprobed with antivinculin antibody, and the quantified intensity of vinculin bands was used to normalize the results of the HA Western blots.

RESULTS

GSK3 specifically phosphorylates residues in the Loop region of p130. The Loop region within the B-pocket domain of p130 contains three pairs of phosphorylated residues matching the consensus pS-X-X-X-pS/pT-P (Fig. 1A) (4). Phosphorylation of two sites (S948 and S982) was shown to be dependent on the priming phosphorylation of S952 and T986 at position +4, respectively (26). GSK3, a ubiquitous serine/threonine protein kinase, preferentially phosphorylates a serine or threonine residue in a position −4 relative to a prephosphorylated S or T residue (21). To test whether GSK3 could phosphorylate the loop of p130 and required a priming phosphorylation, a GST-tagged S935-E1000 fragment of p130 was incubated with recombinant GSK3B and radioactive ATP directly or after prephosphorylation by a proline-directed protein kinase, MAPK1 (13). As shown in Fig. 1B, although GSK3B directly phosphorylated purified GST-Loop fusion protein weakly, this phosphorylation was dramatically facilitated by MAPK1 prephosphorylation.

To test whether GSK3 will specifically phosphorylate full-length p130 protein, wild-type p130 or two mutants carrying alanine substitutions for the potential GSK phosphorylation and priming sites (mutants with sites 1, 3, and 5 changed to A [1,3,5/A] and sites 1 to 6 changed to A [1-6/A]; Fig. 1A) were subjected to GSK3 phosphorylation in vitro. For this experiment, HA-tagged p130 and mutants were transiently expressed in U-2 OS cells, immunoprecipitated with anti-HA antibodies, and incubated in the presence of radioactive γ-ATP and purified GSK3B. As shown in Fig. 1C, wild-type p130 was phosphorylated under these conditions (^{33}P-p130), while either mutant was not. Western blot with anti-HA antibodies revealed equal amount of p130 species in the reactions (Fig. 1C, WB: HA). The GSK3 autophosphorylation was also comparable in all samples (^{33}P-GSK). Therefore, mutation of either putative GSK3 sites (S948, S962, and S982) or priming phosphorylation sites (S952, S966, and T982) abolished phosphorylation of p130 by GSK3 in the context of full-length protein.

To test whether each of the three S-X-X-X-S/T-P sites in the loop of p130 could be phosphorylated by GSK3B, three double mutants where two of three priming phosphorylation sites (S/T-P) were substituted for with alanine (2,4/A, 2,6/A, and 4,6/A), as well as a triple mutant in which all three priming sites were mutated (2,4,6/A), were prepared (Fig. 1). We subjected

these mutants to an in vitro GSK3B phosphorylation as described in the previous experiment and found that while the triple mutant (2,4,6/A) was not phosphorylated under these conditions, the wild-type p130 and each of the double mutants were readily phosphorylated by GSK3B (Fig. 1D). Taken together, these results demonstrate that p130 can serve as a substrate for GSK3 in vitro and that the phosphorylation of p130 by GSK3 at the S948, S962, or S982 sites is dependent on priming phosphorylation at S952, S966, and T986 residues within the Loop.

Inhibition of GSK3 in vivo dramatically affects G_0/G_1 phosphorylation forms of p130. GSK3 kinase activity is present in growth factor-deprived cells (28, 57) when p130 is specifically phosphorylated (4, 22, 38). We tested whether inhibition of GSK3 under the serum-starved conditions would affect phosphorylation of p130. T98G cells were serum starved for 72 h and then treated with 25 mM lithium acetate (47) or 25 μM small-molecule GSK3 inhibitor II (41) for 3 h prior to extraction. For comparison of the p130 phosphorylation status in the control and drug-treated samples, an aliquot of each sample was treated with λ-phosphatase before Western blot analysis. A sample prepared from the cells grown in the presence of 10% serum was used to show the gel migration of hyperphosphorylated form 3 of p130 (Fig. 2A, lanes 1 and 3 or 6). As shown in Fig. 2A, treatment with lithium or inhibitor II led to a marked reduction in gel migration of p130 in serum-starved T98G cells (compare lanes 3 and 4 or 6 and 7). Treatment of the samples with λ-phosphatase resulted in a complete loss of p130 phosphorylation and produced p130 form 1a that migrated identically in untreated and drug-treated series (Fig. 2A, lanes 2, 5, and 8). These results suggest that the difference in gel migration of p130 before and after GSK3 inhibition was phosphorylation related. From this experiment, we conclude that inhibition of GSK3 in serum-starved T98G cells results in a specific loss of G_0/G_1-specific phospho forms of p130.

Next, we tested whether endogenous p130 isolated from serum-starved cells could be phosphorylated by GSK3 in vitro and whether this phosphorylation could be enhanced by pretreatment with a GSK3 inhibitor. T98G cells were serum deprived for 72 h and then treated with 25 mM lithium acetate for 3 h prior to extraction and immunoprecipitation of endogenous p130. Immunoprecipitates were incubated in the presence of radioactive γ-ATP and recombinant GSK3B and analyzed by SDS-PAGE followed by autoradiography and Western blot. As shown in Fig. 2B, the endogenous p130 isolated from G_0/G_1-arrested T98G cells could be specifically phosphorylated by GSK3B. Lithium treatment of the cells enhanced GSK3-dependent phosphorylation 2.5-fold (Fig. 2B, compare lanes 4 and 8 on the ^{33}P-p130 panel). Together with a decrease of p130 G_0/G_1 phosphorylation upon lithium treatment (described above), this result is consistent with specific p130 residues dephosphorylated upon inhibition of GSK3 in vivo that can be rephosphorylated by GSK3B in vitro.

In vivo inhibition of GSK3 by serum stimulation induces a transient loss of the G_0 phosphorylation forms of p130. GSK3 basal activity is high in growth factor-deprived cells and is reduced upon treatment with growth factors through an inhibitory phosphorylation on the serine 21 or serine 9 residue in GSK3A or GSK3B, respectively (10, 21). Given that p130 is phosphorylated in serum-starved cells, we determined whether inhibition of GSK3 upon addition of growth factors would affect p130 phosphorylation. For this experiment, we chose nontransformed human BJ/hTERT fibroblasts (25) immortalized by introduction of human telomerase for their high growth factor dependency and for the absence of the mutations in the components of the growth factor receptor pathways that are often found in cancer cells. BJ/hTERT cells were serum starved for 48 h and then treated with 20% serum and analyzed for the phosphorylation status of endogenous p130 and GSK3B (Fig. 2C and D). Cell cycle progression induced by serum restimulation was monitored by fluorescence-activated cell sorter analysis of DNA (Fig. 2D). Western blot for p130 revealed the presence of phospho form 2 in serum-starved cells (0 h). Starting from 2 h after serum addition, phospho form 2 of p130 became less prominent until it reappeared at 8 h after serum stimulation (Fig. 2C, WB: p130). S9-phosphorylated (pS9, inactive) GSK3B signal was increased immediately after serum addition and then started to decline after 8 h and reached the basal level by 19 to 21 h, while the levels of total GSK3B remained unchanged throughout the experiment (Fig. 2C). Therefore, inhibition of GSK3 induced by serum stimulation of BJ/hTERT cells precedes and coincides with a decrease in the G_0-specific phosphorylation of p130. Interestingly, GSK3B appears to be reactivated as early as at 8 h after serum addition and therefore could potentially contribute to the hyperphosphorylation of p130 during the G_1/S-phase transition (Fig. 2C, WB: p130, form 3).

The decrease in p130 phosphorylation in BJ/hTERT cells after serum addition correlated temporally with the loss of GSK3 activity. To test whether this effect could be detected in other cell types, we serum-starved T98G human glioblastoma cells and mouse NIH 3T3 cell line engineered to express HA-tagged human p130 for 48 h and then treated them either with 20% serum or with 20 mM lithium acetate. As shown in Fig. 2E, the G_0/G_1-specific phospho forms (1 and 2) of both endogenous and HA-tagged p130 were reduced within 3 h of serum or lithium treatment. Further incubation with serum (8 h) resulted in the appearance of hyperphosphorylated p130 species (form 3), while continued lithium treatment led to a sustained decrease in p130 phosphorylation that remained unchanged for up to 24 h (data not shown). Additionally, at the 8-h time point in lithium-treated series, we observed a significant decrease in the p130 protein levels (compare lanes 1 and 2 on Fig. 2E). Taken together, the results presented above strongly indicate that GSK3 contributes to the in vivo phosphorylation of p130 in different cell types.

Phosphorylation of p130 by GSK3 detected by phospho-specific antibodies. To further confirm that GSK3 phosphorylates p130 in vivo, rabbit antibodies were generated against a synthetic peptide containing phosphorylated residues S982 and T986 of human p130 (Fig. 1A). These affinity-purified antibodies (designated ppRb2) could detect endogenous p130 in whole-cell extracts prepared from serum-starved T98G cells and displayed high specificity toward diphosphorylated form of p130. As shown in Fig. 3A, ppRb2 antibodies recognize a protein band comigrating with p130 as detected by the C-terminus-specific antibodies (C-20). In a peptide competition assay, the diphosphorylated pS982/pT986 peptide was able to efficiently block this cross-reactivity (Fig. 3A, lanes 7 to 9), while the nonphosphorylated form of the same peptide was

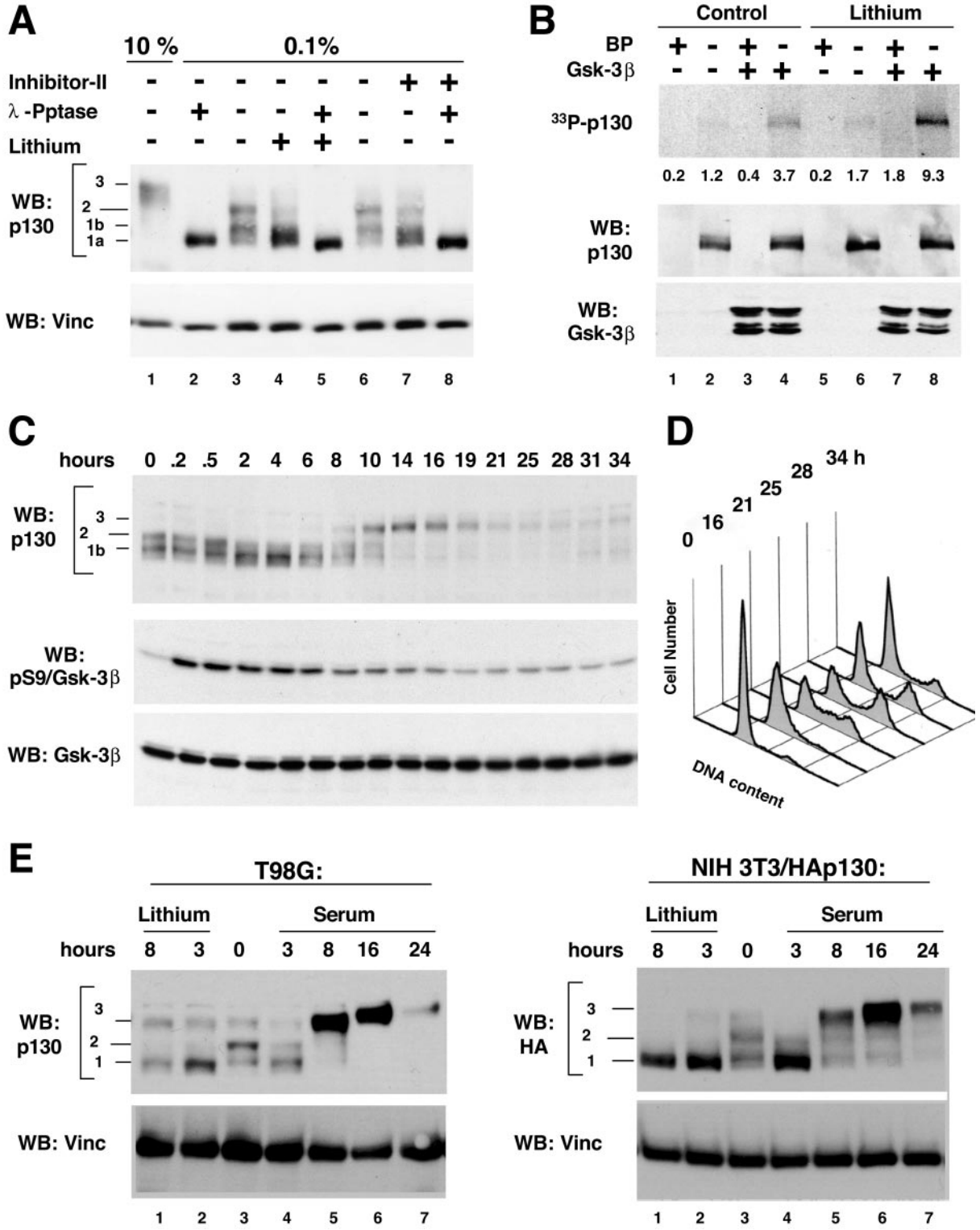

FIG. 2. Inhibition of GSK3 in G_0/G_1-arrested cells leads to a disappearance of specific phospho forms of p130. (A) Inhibition of GSK3 in serum-starved cells results in dephosphorylation of the endogenous p130 in T98G glioblastoma cells. Panel A shows a Western blot (WB) of p130 in extracts prepared from T98G cells that were arrested in G_0 by serum deprivation (lanes 2 to 8) and left untreated (lanes 2 and 3) or treated for 3 h with 25 mM lithium acetate (lanes 4 and 5) or 25 μM GSK3 inhibitor II (lanes 7 and 8). Cell extracts were resolved by SDS-PAGE (6% polyacrylamide gel) prior to blotting onto the nitrocellulose paper. To compare the migration of GSK3 inhibitor-treated and dephosphorylated p130, samples in lanes 2, 5, and 8 were treated with λ-phosphatase (λ-Pptase) prior to loading. A sample prepared from cycling T98G cells (10% FBS, lane 1) is shown to emphasize the difference in gel migration of specific phospho forms of p130 (forms 1a, 1b, 2, and 3, shown to the side). (B) Enhanced GSK3 phosphorylation of p130 from lithium-treated cells compared to intact cells. T98G cells were arrested in G_0 by serum deprivation and left untreated (lanes 1 to 4) or treated for 3 h with 25 mM lithium acetate (lanes 5 to 8) prior to lysis and immunoprecipitation

unable to compete even at a 10-fold-higher concentration (Fig. 3A, lanes 3 to 5). To further test the specificity of the phospho-specific antibodies, a Western blot was performed against the 1,3,5/A and 2,4,6/A mutants of p130. The wild-type p130 and the mutants were expressed in G_0/G_1-arrested NIH 3T3 cells, immunoprecipitated with anti-HA antibody, and Western blotted with ppRb2. Figure 3B (WB: ppRb2) shows that only the wild-type p130, but neither of the mutants, was detected by ppRb2, although all proteins were present in the immunoprecipitates (WB: HA). These experiments strongly suggest that ppRb2 antibody predominantly cross-reacts with p130 that is phosphorylated at serine 982 and threonine 986.

Next, ppRb2 antibodies were used to detect p130 phosphorylation changes upon inhibition of GSK3 in vivo. T98G cells were serum starved for 72 h and then treated for 3 h with the GSK3 inhibitory compounds, lithium acetate and small-molecule inhibitors GSK3 inhibitor II (41), SB-216763, and SB-415286 (9). Unphosphorylated p130 was prepared from an aliquot of T98G extract incubated with λ-phosphatase and served as a control. As shown in Fig. 3C, treatment of the cells with GSK3 inhibitors resulted in a dramatic reduction of ppRb2 recognition of p130 in the cell extracts, similar to that induced by λ-phosphatase treatment of the sample. The total amount of p130 in the extracts was unaffected by the treatments (Fig. 3C, WB: C-20), although the doublet present in the G_0 extracts collapsed to the faster-migrating form 1. This result shows that the loss of ppRb2 recognition could be attributed to a loss of phosphorylation at S982, T986, or both of these sites in p130. Since phosphorylation of T986 site in p130 was previously shown to be CDK dependent and since lithium, SB-216763, and SB-415286 are known not to inhibit other kinases at the concentrations used in this experiment (9, 12), it is most likely that inhibition of GSK3 here induced dephosphorylation of p130 at position S982. However, whether this event could also trigger dephosphorylation of the T986 site via an indirect mechanism remains to be established.

Phosphorylation of the p130 Loop mutants. To determine if the p130 mutants with altered GSK3 and priming phosphorylation sites in the Loop were affected by cell cycle-dependent phosphorylation, we generated stable cell lines expressing HA epitope-tagged wild-type p130 and the mutants of interest. We have previously characterized a p130 deletion mutant lacking the entire Loop region (ΔLoop, with deletion of residues 935 to 997) (4). In addition, we generated several mutants in which specific phosphorylation sites in the Loop were replaced either with alanine to prevent phosphorylation or with aspartic acid residues to mimic a negative charge created by phosphorylation. Using retrovirus-mediated gene transfer followed by antibiotic selection to obtain polyclonal cell populations stably expressing recombinant forms of p130, we generated such cell lines in NIH 3T3 mouse fibroblasts and the T98G human glioblastoma cell background. Ectopic expression of recombinant p130 and mutants resulted in a moderate increase of the total p130 levels that did not affect growth rates of the resulting cell lines (data not shown).

The gel migration patterns of the p130 and phosphorylation site mutants, in which phosphorylation sites in the Loop were substituted for with alanine (1-6/A) or aspartic acid residues (1-6/D), were compared in the NIH 3T3 cells grown in the presence of high (10%) and low (0.1%) percentages of serum. In addition, the serum-starved cell lines were treated with 20 mM lithium acetate for 3 h to test the effect of GSK3 inhibition on the phosphorylation of p130 and mutants. As shown in Fig. 4A, both alanine and aspartic acid substitution in the Loop sites resulted in altered gel migration of p130 both in the presence and in the absence of serum (compare lanes 1, 4, and 7 and lanes 2, 5, and 8). While the wild-type p130 was present as a set of G_0/G_1 forms 1 and 2 that were sensitive to lithium, both 1-6/A and 1-6/D mutants migrated as single bands unaffected by the lithium treatment (lanes 2 and 3, 5 and 6, and 8 and 9). Next, we compared phosphatase sensitivity of the wild-type p130 and mutants expressed in NIH 3T3 cells grown under high- and low-serum conditions. Figure 4B shows an anti-HA Western blot of λ-phosphatase-treated extracts prepared from cells expressing the wild-type p130, 1-6/A, or 1-6/D mutants. Both mutants, as well as the wild-type p130, displayed significant phosphatase sensitivity when expressed under high-serum conditions (lanes 1 to 6), while only the wild-type p130, but not mutants, could be dephosphorylated when extracted from the serum-starved cells (lanes 7 to 12). Insensitivity of the 1-6/A and 1-6/D mutants to the lithium or phosphatase treatment under serum-starved conditions further supports the conclusion that phosphorylation of p130 in G_0/G_1 is specific to the Loop region and is mediated by GSK3. In addition, our data indicate that phosphorylation of the Loop sites contributes to gel migration pattern of form 3 of p130 in proliferating cells (compare lanes 1, 3, and 5, Fig. 4A).

with anti-p130 C-20 antibodies. Control samples were immunoprecipitated in the presence of the C-20 blocking peptide (BP) to ensure the specificity of the reactions (odd lanes). Samples were resolved by SDS-PAGE (7.5% polyacrylamide gel) and transferred to nitrocellulose. The upper panel shows an autoradiogram of p130 (^{33}P-p130) and the PhosphorImager quantification of the p130 signal. Western blot panels of p130 and GSK3B show that equal amounts of these proteins were present in each reaction. (C) Serum restimulation of BJ/hTert fibroblasts results in transient dephosphorylation of p130, coinciding with inactivation of GSK3. BJ/hTert cells were synchronized in G_0 and then treated with 20% serum for the indicated time. Cell extracts were resolved by SDS-PAGE (6% polyacrylamide gel for p130 and 10% polyacrylamide gel for GSK3 analysis, respectively) prior to blotting onto nitrocellulose paper. Western blots show the changes in phosphorylation of p130 occurring during the exit of the cells from the G_0-arrested state and the kinetics of GSK3 inactivation, monitored by phosphorylation of the serine 9 residue (pS9) of GSK3B. The membrane was stripped and reprobed with anti-GSK3B antibodies to ensure equal loading of the samples (Gsk-3β). (D) FACS analysis of DNA content of BJ/hTert cells from the experiment shown on panel C. (E) Serum restimulation results in a transient decrease of G_0/G_1 phosphorylation of p130 in T98G cells, while treatment with lithium leads to a sustained loss of G_0/G_1 phosphorylation. The left panels show a Western blot of p130 in T98G cells that were serum starved for 72 h to induce the G_0/G_1 state (lane 3) and treated with 25 mM lithium acetate (lanes 1 and 2) or 20% fetal calf serum (lanes 4 to 7) for the indicated time. The right panels show a Western blot of the HA-tagged recombinant human p130 stably expressed in NIH 3T3 cells that were serum starved and treated as described above. Cell extracts were resolved by SDS-PAGE (6% polyacrylamide gels) prior to blotting. Membranes were reprobed with antivinculin antibodies to demonstrate equal loading of the samples (WB: Vinc).

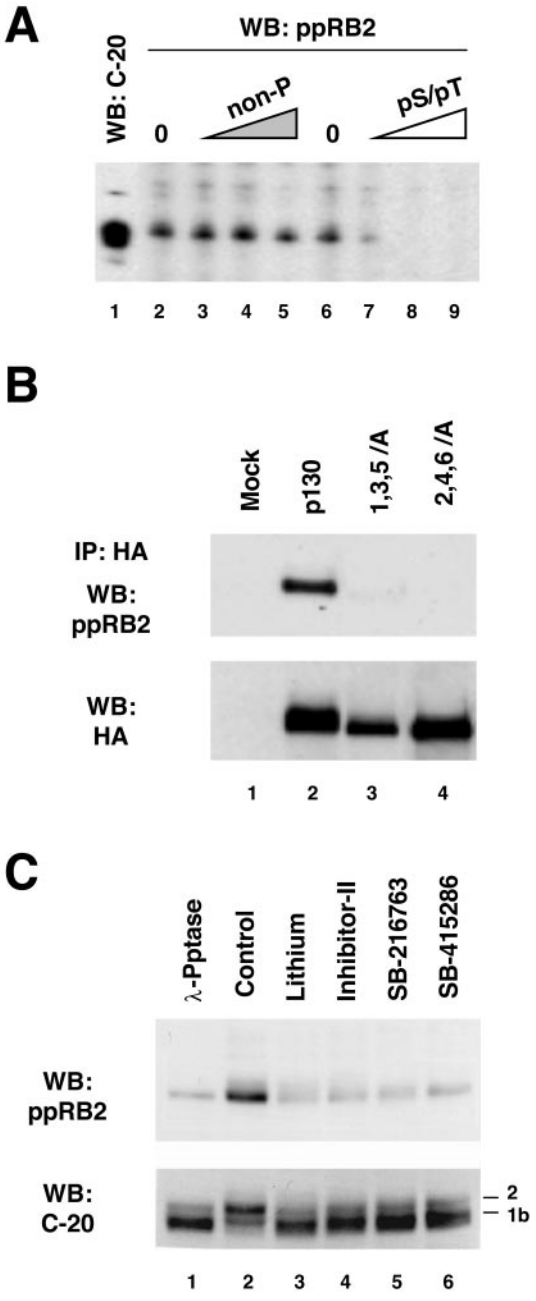

FIG. 3. In vivo phosphorylation of p130 detected by phospho-specific antibodies to GSK3 sites in p130. (A) Characterization of the phospho-specific antibodies raised against pS982/pT986. Whole-cell extract prepared from G_0-arrested T98G cells was run in a preparative single-well gel (7.5% acrylamide), transferred to nitrocellulose, and incubated with the C-20 anti-p130 antibody (lane 1) or ppRb2 phospho-specific anti-p130 antibodies (both at 200 ng/ml) in a multi-slot screening cassette. Phospho-specific antibodies were used directly (lanes 2 and 6) or after preincubation with the indicated blocking peptides. Blocking peptides were used at following concentrations: nonphosphorylated peptide (non-P) at 20, 200, and 2,000 ng/ml and the double-phosphorylated phosphopeptide (pS/pT) at 2, 20, and 200 ng/ml. WB, Western blot. (B) Phospho-specific ppRb2 antibodies do not cross-react with p130 mutants with inactivated GSK3 phosphorylation sites. The top panel shows HA-tagged p130, 1,3,5/A, and 2,4,6/A mutants stably expressed in NIH 3T3 cells, immunoprecipitated (IP) with anti-HA antibodies, resolved by SDS-PAGE (6% polyacrylamide gel), and blotted with ppRb2 antibodies. Parental NIH 3T3 cells were used as a control (lane 1). The cells were arrested by serum deprivation for 48 h prior to the experiment. The blot was reprobed with anti-HA antibody to show comparable amount of proteins in the immunoprecipitates (bottom panel). (C) Inhibition of GSK3 in G_0-arrested cells leads to a decreased recognition of p130 by ppRb2. T98G cells were arrested in G_0 by serum deprivation and left untreated (lanes 1 and 2) or treated with lithium acetate (25 mM, lane 3), GSK3 inhibitor II (25 μM, lane 4), SB-216763 (30 μM, lane 5), or SB-415286 (100 μM, lane 6) for 3 h. Untreated extracts in lane 1 were incubated with λ-phosphatase (λ-Pptase) before loading. The upper panel shows the ppRb2 Western blot of whole-cell extracts resolved by SDS-PAGE (6% polyacrylamide gel). The bottom panel shows the same membrane after stripping and reprobing with C-20 anti-p130 antibody.

Cell cycle-dependent regulation of the p130 Loop mutants. Cell cycle-dependent regulation of p130 includes CDK-mediated phosphorylation and proteosomal degradation in the S phase (26, 37, 54). We observed that HA-tagged p130 stably expressed in NIH 3T3 cells also undergoes cell cycle-dependent phosphorylation and specific changes in its expression levels (Fig. 2E, WB: HA). Similarly to the changes observed for endogenous p130, HA-p130 in NIH 3T3 cells was present as phospho forms 1 and 2 in G_0-arrested cells and as hyperphosphorylated (form 3) at 8 h after serum stimulation and displayed significantly decreased overall expression levels at 24 h (Fig. 2E, WB: p130). To determine whether the Loop contributes to the cell cycle-dependent stability of p130, NIH 3T3 cells expressing p130, 1-6/A or 1-6/D mutants were synchronized in G_0/G_1 and then in early S phase and released to continue the cell cycle and used for Western blot analysis with anti-HA antibody (Fig. 5A). A Western blot for cyclin B1 shown in Fig. 5A serves as a marker of the cell cycle progression, since it is absent in G_0/G_1, expressed in S phase, and degraded upon exit from mitosis. As seen in Fig. 5A, both of the Loop mutants as well as the wild-type p130 underwent phosphorylation in S phase (lanes 2, 8, and 14). Upon completion of the cell cycle (evident from disappearance of cyclin B1), hypo- or unphosphorylated species of p130 and mutants accumulated in all three series (lanes 6, 12, and 18). A decrease in the protein levels upon progression through the S and G_2 phases was also similar in all three series (lanes 4 and 5, 10 and 11, and 16 and 17), although the 1-6/A mutant S/G_2 expression levels were slightly lower than those of the wild type and 1-6/D mutant. This experiment demonstrates that the Loop of p130 is not involved in the cell cycle-dependent regulation of p130, including the changes of the expression levels, hypophosphorylation in G_0 and G_1 and hyperphosphorylation in S phase.

Alanine substitution in the Loop phosphorylation sites in p130 results in a decreased stability of the protein. The expression level of the 1-6/A mutant observed in the cells progressing through the cell cycle was lower than those in the wild-type or 1-6/D p130 (Fig. 5A). We determined whether this mutant had a shorter half-life than the wild-type p130. U-2 OS cells have been previously used to demonstrate the proteosome-mediated degradation of p130 and to determine the half-life of ectopically expressed p130 (54). We generated polyclonal U-2 OS cell lines stably expressing wild-type p130 as well as 1,3,5/A, 1-6/A, or 1-6/D mutants. The cell lines expressed similar levels of the recombinant p130 species, and their growth rates were unaffected by recombinant protein expres-

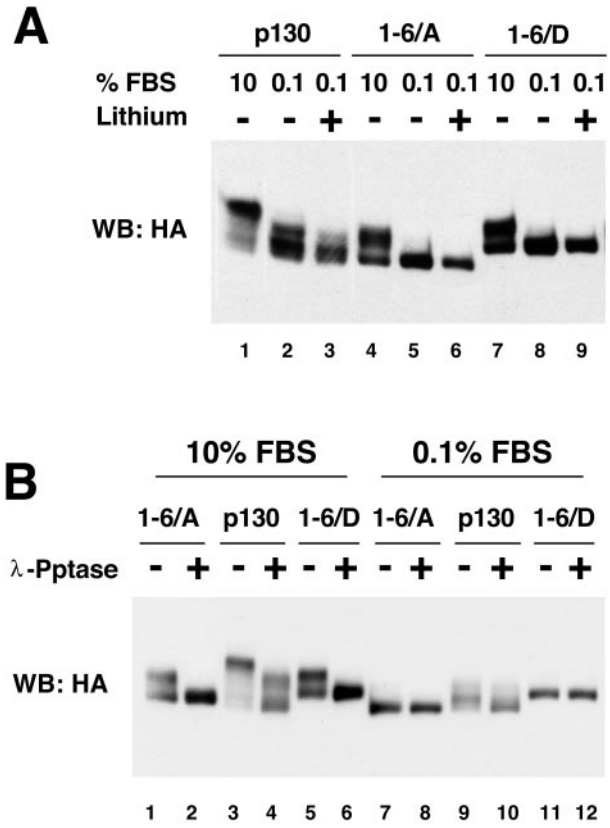

FIG. 4. Characterization of the Loop phosphorylation site mutants of p130. (A) Substitution mutations of the Loop phosphorylation sites in p130 result in an altered gel migration and a loss of lithium sensitivity. NIH 3T3 cells stably expressing HA-tagged p130, 1-6/A, and 1-6/D mutants were grown in standard medium (10% FBS, lanes 1, 4 and 7), serum-starved for 48 h prior to lysis (0.1% FBS, lanes 2, 5, and 8), or serum starved and treated with 25 mM lithium acetate for 3 h prior to lysis (lanes 3, 6, and 9). Lysates were resolved by SDS-PAGE (6% polyacrylamide gel). A Western blot (WB) with anti-HA antibody shows changes in gel migration of p130 and mutants upon treatment. (B) Mutations of the phosphorylation sites in the Loop of p130 result in a loss of phosphatase sensitivity in G_0-arrested but not in cycling cells. A Western blot of HA-tagged p130 and 1-6/A and 1-6/D mutants stably expressed in NIH 3T3 cells and resolved by SDS-PAGE (6% polyacrylamide gel) is shown. The cells were grown in the standard medium (10% FBS, lanes 1 to 6) or arrested by serum deprivation for 48 h prior to lysis (0.1% FBS, lanes 7 to 12). The extracts were incubated with or without λ-phosphatase (λ-Pptase) (odd or even lanes, respectively) prior to loading.

sion (data not shown). Figure 5B (WB: HA) shows a representative Western blot of p130 and the mutants expressed in U-2 OS cells treated with cycloheximide for different times (lanes 1 to 4) or treated for 4 h with cycloheximide and proteosome inhibitor MG132 (33) (lane 5). A graphic representation of the quantitative analysis of p130 and the mutant expression levels determined in at least three independent cycloheximide chase experiments is shown in Fig. 5B, bottom panel. These data demonstrate that the wild-type p130 and 1-6/D mutant displayed similar half-lives significantly exceeding 4 h, while both of the mutants with alanine substitution (1,3,5/A and 1-6/A) had shorter half-lives of approximately 4 h. The proteosome inhibitor MG132, when added together with the cycloheximide, was able to block the degradation of the wild-type p130 as well as the mutants regardless of the status of the Loop. Therefore, phosphorylation of the Loop contributes to stability of p130 without affecting its proteosomal degradation.

DISCUSSION

The cell cycle-dependent phosphorylation of RBL2/p130 has been extensively studied. Recently, 22 serine and threonine residues in p130 were identified that were phosphorylated in vivo (4, 26, 27). Furthermore, it was suggested that three types of kinases, including cyclin D-CDK4/6, cyclin A/E-CDK2, and non-CDK kinase(s), converge to phosphorylate p130 on these residues. Intriguingly, all identified non-CDK phosphorylation sites in p130, including S948, S966, S962, and S982, were clustered in a short nonconserved region within the B-domain (26). Here, we demonstrate that three of these residues, namely S948, S962, and S982, are phosphorylated in vivo by the non-CDK kinase, GSK3. The Loop region of p130, as well as the phosphorylation sites present in the Loop, is not conserved in other pocket proteins, suggesting a unique regulatory role for these phosphorylation sites in p130.

The previous study demonstrated that the non-CDK-dependent phosphorylation at residues S948 and S982 in p130 required priming phosphorylation at CDK-dependent sites (26). Our data here show that GSK3 phosphorylation of p130 Loop can be enhanced by priming phosphorylation by a proline-directed kinase (MAPK1) in vitro (Fig. 1B). Moreover, the finding that GSK3 phosphorylation of full-length p130 was equally efficiently blocked by either the combined mutation of the S948, S962, and S982 phosphorylation sites in the Loop or S952, S966, and T986 sites (Fig. 1C) strongly supports a priming phosphorylation-dependent mechanism of GSK3 phosphorylation of p130. Priming-dependent phosphorylation is characteristic for many known substrates of GSK3, including the classical substrate glycogen synthase (10, 21, 55, 57). Such a mechanism creates a basis for an involvement of GSK3 in regulation of a diverse variety of cellular proteins and provides specificity of the regulation of GSK3 substrates by integrating multiple signaling pathways. It remains unclear whether CDKs could mediate the priming phosphorylation of the p130 Loop sites in the context of the G_0/G_1-arrested cells where CDK activity is dramatically down-regulated or whether other proline-directed kinases could be responsible for this phosphorylation. Since a significant part if not all of the p130 protein pool undergoes proteosomal degradation in S phase of the cell cycle (54), the second possibility appears more likely. Another intriguing question that remained outside the scope of this study is whether GSK3 that appears only transiently inactivated upon serum restimulation of the serum-starved G_0/G_1-arrested cells (Fig. 2C) could contribute to the hyperphosphorylation of p130 in late G_1/S phase.

To study the functional role of the p130 Loop phosphorylation, we created stable cell lines ectopically expressing moderate levels of recombinant p130 proteins. Initial characterization of the p130-expressing cell lines revealed that the recombinant p130 undergoes cell cycle-dependent regulation similar to the endogenous p130 protein, including the changes in phosphorylation and expression levels. Therefore, this ex-

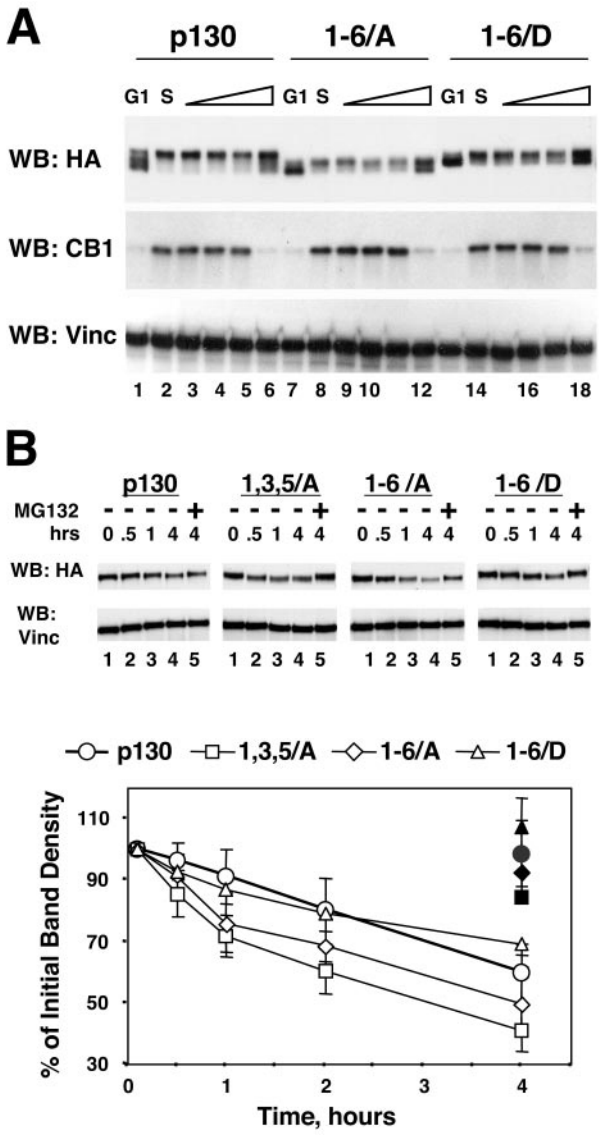

FIG. 5. Cell cycle-dependent expression of the Loop phosphorylation site mutants of p130. (A) Phosphorylation site mutants of the Loop of p130 expressed in NIH 3T3 cells undergo cell cycle-dependent changes. NIH 3T3 cells stably expressing HA-tagged p130, 1-6/A, or 1-6/D mutants were arrested in G_0/G_1 by serum deprivation (lanes 1, 7, and 13) and further synchronized in early S phase by incubation for 16 h with medium supplemented with 20% FBS and 1 mM hydroxyurea (lanes 2, 8, and 14). The medium was then replaced with standard growth medium (10% FBS), and the cells were allowed to continue the cell cycle for an additional 2, 4, 6, or 10 h (lanes 3 to 6, 9 to 12, and 15 to 18). The upper panel shows a Western blot (WB) of p130 and mutants detected with anti-HA antibody, the middle panel is a Western blot of cyclin B1, and the bottom panel shows the same membrane stripped and reprobed with antivinculin (Vinc) antibody to confirm equal loading of the samples. (B) Alanine substitution in the Loop phosphorylation sites in p130 results in a decreased stability of mutant proteins. U-2 OS cells stably expressing HA-tagged p130 and the indicated mutants were incubated for 0, 0.5, 1, and 4 h with cycloheximide (lanes 1 to 4) or for 4 h with cycloheximide and proteosome inhibitor MG132 (33) (lane 5). Expression of p130 and the mutants was analyzed by SDS-PAGE (10% polyacrylamide gels) followed by Western blot with anti-HA antibody and quantitatively evaluated by densitometry. Representative Western blots are shown in the top panel. The same membrane was stripped and reprobed with antivinculin antibody to ensure equal loading of the samples. The amount of p130 was normalized by vinculin and expressed as a percentage of the value taken at time zero. Filled symbols on the graph show the values of the corresponding MG132-treated series. The graph shows average values and standard deviation of at least three experiments.

perimental system allowed us to study the regulation of mutant p130 proteins in the context of the cell cycle and to analyze their functional interactions while avoiding overexpression conditions that could result in artifacts. Using NIH 3T3 cells stably expressing phosphorylation site mutants of p130, we found that the alanine or aspartic acid substitution of the phosphorylated residues in the Loop (1-6/A or 1-6/D, Fig. 1A) (4) results in a complete loss of the G_0/G_1-specific phosphorylation of the mutant p130 proteins (Fig. 4). These mutants, however, were able to undergo CDK-dependent phosphorylation both in asynchronous cells and in synchronized cells upon the G_1/S transition (Fig. 4 and 5A). This result is in agreement with the previously reported p130 mutagenesis data where the alanine substitution in 12 phosphorylation sites (including 6 residues in the Loop region) did not affect the phosphorylation of the remaining 9 sites (19).

We also used the p130 stable cell lines to test whether the Loop phosphorylation is essential for interactions of p130 with its known cellular partners. Alanine substitution in some or all phosphorylation sites in the Loop region of p130 does not affect its ability to interact with E2F4 in transient transfection experiments (4, 19, 26). However, given that the Loop sites in p130 were clearly phosphorylated in G_0/G_1-arrested cells where p130 is predominantly associated with E2F4, we tested the possibility of whether the mutation mimicking the "constantly phosphorylated" state of the Loop will result in more efficient or sustained binding of p130 with E2F4. Using stable cell lines expressing 1-6/A or 1-6/D mutants of p130 to monitor their interaction with E2F4 in the context of the cell cycle, we did not observe any differences in the efficiency or the dynamics of this binding (unpublished data). Unlike pRb, which exhibits its growth suppression activity mainly through the repression of E2Fs, both p107 and p130 are able to block the cell cycle progression by binding cyclin A- or E-CDK2 complexes that has been shown to inhibit the activity of these kinase complexes (reviewed in references 6 and 24). While the p130 mutagenesis study published previously found the binding of cyclin A or E with p130 to be phosphorylation independent (26), another report suggested that cyclins A and E could preferentially bind to specific phosphorylated forms of p130 in the endogenous immunoprecipitation experiments (30). We found that both 1-6/A and 1-6/D mutants were able to bind cyclins similarly to the wild-type p130 (unpublished data). In addition, we were able to detect both E2F4 and cyclin E in the cell-cycle-specific complexes with endogenous p130 immunoprecipitated with the phospho-specific ppRb2 antibodies (unpublished data). Our results therefore demonstrate that interaction of p130 with E2F4 and G_1/S cyclins is not affected by phosphorylation status of the Loop.

Transformation of certain cell types by SV40 large T antigen is mediated in part by interaction of T antigen with retinoblastoma family proteins, including p107 and p130 (59). This interaction has been shown to be dependent on the integrity of the LXCXE motif in T antigen and a subset of conserved

amino acid residues in the B-domain of pocket proteins (Y709 and K713 in pRb and Y879 and K901 in p130) (5, 15, 59). We hypothesized that close proximity of the highly phosphorylated Loop region could influence the interaction between T antigen and p130. However, both 1-6/A and 1-6/D mutants of p130 as well as the ΔLoop mutant were able to bind to T antigen, demonstrating that an intact Loop is not required for this interaction (unpublished data).

The Loop region of p130 contains a functional nuclear localization signal, ^{935}KRKRR^{939} (5), located in the vicinity of the GSK3 phosphorylation sites. Phosphorylation of cyclin D1 by GSK3 promotes its nuclear export (16). We looked into cellular localization of p130 mutants where phosphorylation sites in the Loop were replaced with alanine (1,3,5/A and 1-6/A) or aspartic acid residues (1-6/D) and could not detect any differences in nuclear localization of these p130 mutants (unpublished data). Additionally, we have previously found that p130 accumulates in the cytoplasm upon G_1/S transition due to the nuclear export (5). Given the possibility that GSK3 could be reactivated in S phase, we tested whether 1-6/A mutations or 1-6/D mutations in the Loop would affect nuclear export of p130. We found that the nucleocytoplasmic distribution of the p130 Loop mutants was very similar to that of the wild-type p130 in synchronized cells (unpublished data), indicating that both nuclear localization of p130 and its nuclear export in S phase were independent of the phosphorylation status of the Loop.

In summary, the results discussed above demonstrate that the Loop region in the B pocket of p130 harbors residues that are responsible for G_0/G_1 phosphorylation of p130. This region, however, is not essential for the known functions of p130 associated with its ability to block the cell cycle progression, including interaction with E2F4, cyclins A and E, and the LXCXE-containing proteins. However, we found that the stability of p130 mutants where the Loop could not be phosphorylated (1,3,5/A and 1-6/A) was modestly reduced compared to that of the wild-type p130 (Fig. 5B and C). p130 has been shown to be targeted to proteosomal degradation by SCF^{SKP2} ubiquitin-ligase complex, and this degradation is thought to be triggered by phosphorylation of p130 by CDK4/6 at S972 in the spacer domain (2, 54). Our results show that the degradation of the wild-type p130, as well as the Loop phosphorylation site mutants 1,3,5/A, 1-6/A, and 1-6/D, was inhibited by the treatment of cells with proteosomal inhibitor (Fig. 5B and C), suggesting that the degradation of all p130 species occurred in proteosome-dependent manner. We also observed that the levels of 1-6/A and 1-6/D mutant proteins were high in G_0/G_1-arrested cells, reduced upon the S-phase progression, and then up-regulated again as the cells entered G_1 phase, indicating their susceptibility to the cell cycle-dependent proteosomal degradation (Fig. 5A). GSK3 phosphorylation has been shown to decrease the stability of and target to proteosomal degradation several proteins implicated in cellular proliferation, including c-Myc (50), cyclin D1 (16), and β-catenin (49). Accumulation of these GSK3 substrates in the cells is linked to increased proliferation and is observed in different types of cancer. It is yet unclear whether the observed destabilization of a nonphosphorylated Loop mutant of p130 indicates an additional, proteosome-independent mechanism of regulation of p130 expression levels. We should point out that the effect of 1,3,5/A and 1-6/A mutations on the stability of p130 appears modest and could result from conformational changes. The fact that unlike the other GSK3 substrates mentioned above, destabilization of p130 was caused by lack of phosphorylation at the GSK3-targeted fragment indicates a novel way of GSK3-mediated regulation. Interestingly, a regulatory component of the adenomatous polyposis coli–β-catenin complex, axin, has been shown to be phosphorylated by GSK3, and this phosphorylation resulted in its stabilization while alanine substitution in the putative GSK3 sites resulted in destabilization of the mutant protein (58). To our knowledge, this is the only other example of stabilization of substrate protein caused by GSK3 phosphorylation besides our result from p130 described here. It would be intriguing to find out whether there is a common mechanism that regulates these two GSK3 targets.

Our data presented here identify p130 as a novel target of GSK3, adding to the list of the GSK3 substrates implicated into the control of cell proliferation. While we did not find a link between GSK3 phosphorylation of p130 and any known cell cycle regulatory functions of p130 or the cell cycle-dependent regulation of p130, our work sets the stage for further studies aimed at elucidating the physiological functions of these two intriguing proteins.

ACKNOWLEDGMENTS

We are grateful to William Hahn, Ralph Scully, and Hartmut Land for reagents.

This work was supported in part by Public Health Service grant RO1-CA63113 (J.D.).

REFERENCES

1. **Ausubel, F. M. (ed.).** 1999. Short protocols in molecular biology, 4th ed. John Wiley & Sons, Inc., New York, N.Y.
2. **Bhattacharya, S., J. Garriga, J. Calbo, T. Yong, D. S. Haines, and X. Grana.** 2003. SKP2 associates with p130 and accelerates p130 ubiquitylation and degradation in human cells. Oncogene **22:**2443–2451.
3. **Cam, H., and B. D. Dynlacht.** 2003. Emerging roles for E2F: beyond the G1/S transition and DNA replication. Cancer Cell **3:**311–316.
4. **Canhoto, A. J., A. Chestukhin, L. Litovchick, and J. A. DeCaprio.** 2000. Phosphorylation of the retinoblastoma-related protein p130 in growth-arrested cells. Oncogene **19:**5116–5122.
5. **Chestukhin, A., L. Litovchick, K. Rudich, and J. A. DeCaprio.** 2002. Nucleocytoplasmic shuttling of p130/RBL2: novel regulatory mechanism. Mol. Cell. Biol. **22:**453–468.
6. **Classon, M., and N. Dyson.** 2001. p107 and p130: versatile proteins with interesting pockets. Exp. Cell Res. **264:**135–147.
7. **Classon, M., S. Salama, C. Gorka, R. Mulloy, P. Braun, and E. Harlow.** 2000. Combinatorial roles for pRB, p107, and p130 in E2F-mediated cell cycle control. Proc. Natl. Acad. Sci. USA **97:**10820–10825.
8. **Cobrinik, D., M. H. Lee, G. Hannon, G. Mulligan, R. T. Bronson, N. Dyson, E. Harlow, D. Beach, R. A. Weinberg, and T. Jacks.** 1996. Shared role of the pRB-related p130 and p107 proteins in limb development. Genes Dev. **10:**1633–1644.
9. **Coghlan, M. P., A. A. Culbert, D. A. Cross, S. L. Corcoran, J. W. Yates, N. J. Pearce, O. L. Rausch, G. J. Murphy, P. S. Carter, L. Roxbee Cox, D. Mills, M. J. Brown, D. Haigh, R. W. Ward, D. G. Smith, K. J. Murray, A. D. Reith, and J. C. Holder.** 2000. Selective small molecule inhibitors of glycogen synthase kinase-3 modulate glycogen metabolism and gene transcription. Chem. Biol. **7:**793–803.
10. **Dajani, R., E. Fraser, S. M. Roe, N. Young, V. Good, T. C. Dale, and L. H. Pearl.** 2001. Crystal structure of glycogen synthase kinase 3 beta: structural basis for phosphate-primed substrate specificity and autoinhibition. Cell **105:**721–732.
11. **Dannenberg, J. H., A. van Rossum, L. Schuijff, and H. te Riele.** 2000. Ablation of the retinoblastoma gene family deregulates G(1) control causing immortalization and increased cell turnover under growth-restricting conditions. Genes Dev. **14**:3051–3064.
12. **Davies, S. P., H. Reddy, M. Caivano, and P. Cohen.** 2000. Specificity and mechanism of action of some commonly used protein kinase inhibitors. Biochem. J. **351:**95–105.
13. **Davis, R. J.** 1993. The mitogen-activated protein kinase signal transduction pathway. J. Biol. Chem. **268:**14553–14556.

14. **DeCaprio, J. A., J. W. Ludlow, J. Figge, J. Y. Shew, C. M. Huang, W. H. Lee, E. Marsilio, E. Paucha, and D. M. Livingston.** 1988. SV40 large tumor antigen forms a specific complex with the product of the retinoblastoma susceptibility gene. Cell **54:**275–283.
15. **Dick, F. A., E. Sailhamer, and N. J. Dyson.** 2000. Mutagenesis of the pRB pocket reveals that cell cycle arrest functions are separable from binding to viral oncoproteins. Mol. Cell. Biol. **20:**3715–3727.
16. **Diehl, J. A., M. Cheng, M. F. Roussel, and C. J. Sherr.** 1998. Glycogen synthase kinase-3beta regulates cyclin D1 proteolysis and subcellular localization. Genes Dev. **12:**3499–3511.
17. **Dyson, N.** 1998. The regulation of E2F by pRB-family proteins. Genes Dev. **12:**2245–2262.
18. **Dyson, N., K. Buchkovich, P. Whyte, and E. Harlow.** 1989. The cellular 107K protein that binds to adenovirus E1A also associates with the large T antigens of SV40 and JC virus. Cell **58:**249–255.
19. **Farkas, T., K. Hansen, K. Holm, J. Lukas, and J. Bartek.** 2002. Distinct phosphorylation events regulate p130- and p107-mediated repression of E2F4. J. Biol. Chem. **277:**26741–26752.
20. **Ferkey, D. M., and D. Kimelman.** 2000. GSK3: new thoughts on an old enzyme. Dev. Biol. **225:**471–479.
21. **Frame, S., P. Cohen, and R. M. Biondi.** 2001. A common phosphate binding site explains the unique substrate specificity of GSK3 and its inactivation by phosphorylation. Mol. Cell **7:**1321–1327.
22. **Garriga, J., A. Limon, X. Mayol, S. G. Rane, J. H. Albrecht, E. P. Reddy, V. Andres, and X. Grana.** 1998. Differential regulation of the retinoblastoma family of proteins during cell proliferation and differentiation. Biochem. J. **333:**645–654.
23. **Ghosh, M. K., and M. L. Harter.** 2003. A viral mechanism for remodeling chromatin structure in G0 cells. Mol. Cell **12:**255–260.
24. **Graña, X., J. Garriga, and X. Mayol.** 1998. Role of the retinoblastoma protein family, pRB, p107 and p130 in the negative control of cell growth. Oncogene **17:**3365–3383.
25. **Hahn, W. C., C. M. Counter, A. S. Lundberg, R. L. Beijersbergen, M. W. Brooks, and R. A. Weinberg.** 1999. Creation of human tumour cells with defined genetic elements. Nature **400:**464–468.
26. **Hansen, K., T. Farkas, J. Lukas, K. Holm, L. Ronnstrand, and J. Bartek.** 2001. Phosphorylation-dependent and -independent functions of p130 cooperate to evoke a sustained G1 block. EMBO J. **20:**422–432.
27. **Hansen, K., J. Lukas, K. Holm, A. A. Kjerulff, and J. Bartek.** 1999. Dissecting functions of the retinoblastoma tumor suppressor and the related pocket proteins by integrating genetic, cell biology, and electrophoretic techniques. Electrophoresis **20:**372–381.
28. **Harwood, A. J.** 2001. Regulation of GSK3: a cellular multiprocessor. Cell **105:**821–824.
29. **Herrera, R. E., V. P. Sah, B. O. Williams, T. P. Mäkelä, R. A. Weinberg, and T. Jacks.** 1996. Altered cell cycle kinetics, gene expression, and G_1 restriction point regulation in *Rb*-deficient fibroblasts. Mol. Cell. Biol. **16:**2402–2407.
30. **Lacy, S., and P. Whyte.** 1997. Identification of a p130 domain mediating interactions with cyclin A/cdk 2 and cyclin E/cdk 2 complexes. Oncogene **14:**2395–2406.
31. **LeCouter, J. E., B. Kablar, W. R. Hardy, C. Ying, L. A. Megeney, L. L. May, and M. A. Rudnicki.** 1998. Strain-dependent myeloid hyperplasia, growth deficiency, and accelerated cell cycle in mice lacking the Rb-related *p107* gene. Mol. Cell. Biol. **18:**7455–7465.
32. **LeCouter, J. E., B. Kablar, P. F. Whyte, C. Ying, and M. A. Rudnicki.** 1998. Strain-dependent embryonic lethality in mice lacking the retinoblastoma-related p130 gene. Development **125:**4669–4679.
33. **Lee, D. H., and A. L. Goldberg.** 1996. Selective inhibitors of the proteasome-dependent and vacuolar pathways of protein degradation in Saccharomyces cerevisiae. J. Biol. Chem. **271:**27280–27284.
34. **Lee, M. H., B. O. Williams, G. Mulligan, S. Mukai, R. T. Bronson, N. Dyson, E. Harlow, and T. Jacks.** 1996. Targeted disruption of p107: functional overlap between p107 and Rb. Genes Dev. **10:**1621–1632.
35. **Li, Y., C. Graham, S. Lacy, A. M. Duncan, and P. Whyte.** 1993. The adenovirus E1A-associated 130-kD protein is encoded by a member of the retinoblastoma gene family and physically interacts with cyclins A and E. Genes Dev. **7:**2366–2377.
36. **Lipinski, M. M., and T. Jacks.** 1999. The retinoblastoma gene family in differentiation and development. Oncogene **18:**7873–7882.
37. **Mayol, X., J. Garriga, and X. Graña.** 1995. Cell cycle-dependent phosphorylation of the retinoblastoma-related protein p130. Oncogene **11:**801–808.
38. **Mayol, X., J. Garriga, and X. Graña.** 1996. G1 cyclin/CDK-independent phosphorylation and accumulation of p130 during the transition from G1 to G0 lead to its association with E2F4. Oncogene **13:**237–246.
39. **Morgenstern, J. P., and H. Land.** 1990. Advanced mammalian gene transfer: high titre retroviral vectors with multiple drug selection markers and a complementary helper-free packaging cell line. Nucleic Acids Res. **18:**3587–3596.
40. **Mulligan, G., and T. Jacks.** 1998. The retinoblastoma gene family: cousins with overlapping interests. Trends Genet. **14:**223–229.
41. **Naerum, L., L. Norskov-Lauritsen, and P. H. Olesen.** 2002. Scaffold hopping and optimization towards libraries of glycogen synthase kinase-3 inhibitors. Bioorg. Med. Chem. Lett. **12:**1525–1528.
42. **Pear, W. S., G. P. Nolan, M. L. Scott, and D. Baltimore.** 1993. Production of high-titer helper-free retroviruses by transient transfection. Proc. Natl. Acad. Sci. USA **90:**8392–8396.
43. **Plyte, S. E., K. Hughes, E. Nikolakaki, B. J. Pulverer, and J. R. Woodgett.** 1992. Glycogen synthase kinase-3: functions in oncogenesis and development. Biochim. Biophys. Acta **1114:**147–162.
44. **Reynolds, C. H., J. C. Betts, W. P. Blackstock, A. R. Nebreda, and B. H. Anderton.** 2000. Phosphorylation sites on tau identified by nanoelectrospray mass spectrometry: differences in vitro between the mitogen-activated protein kinases ERK2, c-Jun N-terminal kinase and P38, and glycogen synthase kinase-3beta. J. Neurochem. **74:**1587–1595.
45. **Rossi, F., H. E. MacLean, W. Yuan, R. O. Francis, E. Semenova, C. S. Lin, H. M. Kronenberg, and D. Cobrinik.** 2002. p107 and p130 coordinately regulate proliferation, Cbfa1 expression, and hypertrophic differentiation during endochondral bone development. Dev. Biol. **247:**271–285.
46. **Ruiz, S., C. Segrelles, A. Bravo, M. Santos, P. Perez, H. Leis, J. L. Jorcano, and J. M. Paramio.** 2003. Abnormal epidermal differentiation and impaired epithelial-mesenchymal tissue interactions in mice lacking the retinoblastoma relatives p107 and p130. Development **130:**2341–2353.
47. **Ryves, W. J., and A. J. Harwood.** 2001. Lithium inhibits glycogen synthase kinase-3 by competition for magnesium. Biochem. Biophys. Res. Commun. **280:**720–725.
48. **Sage, J., G. J. Mulligan, L. D. Attardi, A. Miller, S. Chen, B. Williams, E. Theodorou, and T. Jacks.** 2000. Targeted disruption of the three Rb-related genes leads to loss of G(1) control and immortalization. Genes Dev. **14:**3037–3050.
49. **Salic, A., E. Lee, L. Mayer, and M. W. Kirschner.** 2000. Control of beta-catenin stability: reconstitution of the cytoplasmic steps of the wnt pathway in Xenopus egg extracts. Mol. Cell **5:**523–532.
50. **Sears, R., F. Nuckolls, E. Haura, Y. Taya, K. Tamai, and J. R. Nevins.** 2000. Multiple Ras-dependent phosphorylation pathways regulate Myc protein stability. Genes Dev. **14:**2501–2514.
51. **Smith, E. J., G. Leone, J. DeGregori, L. Jakoi, and J. R. Nevins.** 1996. The accumulation of an E2F-p130 transcriptional repressor distinguishes a G_0 cell state from a G_1 cell state. Mol. Cell. Biol. **16:**6965–6976.
52. **Smith, E. J., G. Leone, and J. R. Nevins.** 1998. Distinct mechanisms control the accumulation of the Rb-related p107 and p130 proteins during cell growth. Cell Growth Differ. **9:**297–303.
53. **Stevaux, O., and N. J. Dyson.** 2002. A revised picture of the E2F transcriptional network and RB function. Curr. Opin. Cell Biol. **14:**684–691.
54. **Tedesco, D., J. Lukas, and S. I. Reed.** 2002. The pRb-related protein p130 is regulated by phosphorylation-dependent proteolysis via the protein-ubiquitin ligase SCF(Skp2). Genes Dev. **16:**2946–2957.
55. **ter Haar, E., J. T. Coll, D. A. Austen, H. M. Hsiao, L. Swenson, and J. Jain.** 2001. Structure of GSK3beta reveals a primed phosphorylation mechanism. Nat. Struct. Biol. **8:**593–596.
56. **Whyte, P., K. J. Buchkovich, J. M. Horowitz, S. H. Friend, M. Raybuck, R. A. Weinberg, and E. Harlow.** 1988. Association between an oncogene and an anti-oncogene: the adenovirus E1A proteins bind to the retinoblastoma gene product. Nature **334:**124–129.
57. **Woodgett, J. R.** 2001. Judging a protein by more than its name: GSK3. Sci. STKE **2001:**RE12. [Online.] http://stke.sciencemag.org.
58. **Yamamoto, H., S. Kishida, M. Kishida, S. Ikeda, S. Takada, and A. Kikuchi.** 1999. Phosphorylation of axin, a Wnt signal negative regulator, by glycogen synthase kinase-3beta regulates its stability. J. Biol. Chem. **274:**10681–10684.
59. **Zalvide, J., and J. A. DeCaprio.** 1995. Role of pRb-related proteins in simian virus 40 large-T-antigen-mediated transformation. Mol. Cell. Biol. **15:**5800–5810.
60. **Zhang, S., X. Qian, C. Redman, V. Bliskovski, E. S. Ramsay, D. R. Lowy, and B. A. Mock.** 2003. p16 INK4a gene promoter variation and differential binding of a repressor, the ras-responsive zinc-finger transcription factor, RREB. Oncogene **22:**2285–2295.
61. **Zhang, S., E. S. Ramsay, and B. A. Mock.** 1998. Cdkn2a, the cyclin-dependent kinase inhibitor encoding p16INK4a and p19ARF, is a candidate for the plasmacytoma susceptibility locus, Pctr1. Proc. Natl. Acad. Sci. USA **95:**2429–2434.